On the Full Stand Modeling and Tension Control for the Hot Strip Finishing Mill with PID Structure

Byoung Joon Ahn
Department of Mechanical and Intelligent Systems Engineering, Pusan National University, JangJeon-Dong, KumJeong-Ku, Pusan 609-735, Korea
Ju Yong Choi
Department of Mechanical and Intelligent Systems Engineering, Pusan National University, JangJeon-Dong, KumJeong-Ku, Pusan 609-735, Korea
Yu Shin Chang
Department of Mechanical and Intelligent Systems Engineering, ERC/NSDM Pusan National University, JangJeon-Dong, KumJeong-Ku, Pusan 609-735, Korea
Man Hyung Lee*
School of Mechanical Engineering, Pusan National University, JangJeon-Dong, KumJeong-Ku, Pusan 609-735, Korea

We describe a looper controller design for a hot strip finishing mill in steel plants. The main function of the looper system is to balance the mass flow of the strip by accumulating material in the middle of the stands. Another function is to control the strip tension which influences the width of the strip. To ensure strip quality, it is very important to control the tension of the hot strip finishing mill. However, because there is a mutual interaction between the looper angle and the strip tension, it is difficult to control the looper system. Previous researches examined only the operation of a single stand. But it is not sufficient to examine the operation and effect of whole stands because the operation is wholly interdependent. In this paper, we present a full model of the hot strip finishing mill in order to more effectively control strip tension. We propose several control methods for the full-stand hot strip finishing mill, denoted as conventional PI, PI with cross gain, and coefficient diagram method (CDM) PID control. In the real plants, there are some problems by using higher order controllers such as LQ, LQG and H_∞. By comparison, the PID controller is very simple and easy to apply to all real plants. To that end, we present our findings on PID controls and their potential use in the hot strip finishing mill.

Key Words: Hot Strip Finishing Mill, Tension, Looper System, Conventional PI, Cross Control, CDM

1. Introduction

In the hot strip finishing mill process, width-control is extremely important in satisfying customer demand. Uniform width of the strip is regarded highly desired because it reduces strip trimming and improves efficiency of the strip. The final strip width is determined by the finishing mill which consists of several processing stands. When the speed of the strip between adjacent stands varies, excessive or poor tension occurs in the strip and, consequently, irregular strip-width appears along the strip length. Thus appropriate

* Corresponding Author,
E-mail : mahlee@pusan.ac.kr
TEL : +82-51-510-2331; **FAX** : +82-51-512-9835
School of Mechanical Engineering, Pusan National University, JangJeon-Dong, KumJeong-Ku, Pusan 609-735, Korea. (Manuscript **Received** June 16, 2003; **Revised** May 3, 2004)

tension must be maintained by using the looper system to prevent excessive or poor tension in the hot strip finishing mill. The main function of the looper system is to regulate the mass flow of the strip by accumulating as well as releasing the strip between the stands. Another function of the system is to control the strip tension which influences the width of the strip. However it is difficult to control the tension independently because there is interaction between the tension and the angle of the looper. Other problems caused by the rolling process include temperature, stiffness, deformation, etc., all or any of which may effect negatively on the system.

To solve these problems, most research on tension control for the looper system has investigated the means of non-interacting control. This single stand research has led to many advances in milling. And the adoptions of PID, Cross control with PID, LQ and H_∞ have been announced (Lee, 2001 ; Hesketh et al., 1998). Nonetheless, such studies are limited because they deal only with a single stand system (i.e., one looper system between adjacent two stands) (Hearns and Grimble, 1997 ; Masanoti Shioya et al., 1995 ; Myungjun, 1998). In reality, however, almost all hot strip finishing mill process is composed of seven stands and 6 loopers placed between the adjacent stands, as shown in Fig. 1. Moreover, all the looper systems interact with the adjacent stands. So, because of the interactions, the analysis of a single stand cannot adequately describe the full process. Thus, to determine the totality of the interactions, a full stand model needs to be studied.

In this paper, the interaction of all the stands of the finishing mill are analyzed and the controller,

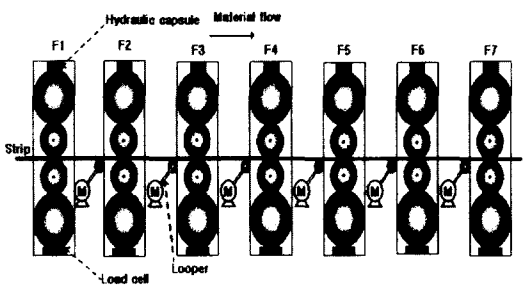

Fig. 1 Hot finishing mill process

which is obtained from each single stand, is expanded to incorporate the operation of all 7 stands. We will show simulation results of the Conventional PI control for full stands and Cross control with appropriate tuning methods for full stands. Furthermore, we will take advantage of another PID controller known as the CDM, announced by S. Manabe (1997, 1998) and apply it to the system by Young-Chol Kim (2001). Another reason to adopt the PID structured controller is that in the real plants, problems are typically encountered when using higher order controllers such as LQ, LQG and H_∞. However, the PID controller is very simple and readily applicable to all practical plants ; in particular, it can transcend the regulation limitations of higher order controller such as LQ, LQG and H_∞. In order to realize this potential, we will discuss some PID controllers for the finishing mill plant and their properties. Our findings can be applied to a hot strip finishing mill plant simulator which uses a full stand model.

2. Modeling of Hot Strip Finishing Mill

2.1 Modeling of single stand

Figure 1 shows that the hot strip finishing mill consists of seven stands and six loopers which maintain the uniform tension among the set of work rolls. In the finishing mill, the main motor drives the work rolls, so the strip flow is produced and controlled by the main motor. The looper motor drives the looper system and maintains the torque, so that the strip tension can be regulated.

First, appropriate modeling is needed to control the finishing mill. In order to produce a modeling of the seven stands of the hot strip finishing mill process, we simulated a total system by extrapolating from the modeling of a single stand. Figure 2 represents the single stand model. The non-linear dynamic equation is obtained by the equations of the geometric structure shown in Fig. 2. For a more detailed derivation and the meaning of each term, it is useful to Ref. (Hearns and Grimble, 1997). The results are as follows.

$$t_f=\frac{E}{L_0}(F_2(\theta)-\xi(t))$$

$$\dot{\theta}(t)=\frac{1}{g_L}\omega(t)$$

$$\dot{\omega}(t)=-\frac{F_3(t_f)}{J_L}t_f(t)-\frac{z}{J_L}\omega(t)+\frac{1}{J_L}\tau(t)-\frac{1}{J_L}(T_s(\theta)+T_L(\theta))$$

$$\dot{\tau}(t)=\frac{1}{T_2}\tau_{ref}(t)-\frac{1}{T_2}\tau(t)$$

$$\dot{V}_r(t)=-\frac{1}{T_v}V_r(t)+\frac{1}{T_v}V_{r\_ref}(t)$$

$$\dot{t}_f=-\frac{E}{L_0}K_{10}t_f+\frac{E}{L_0\cdot g_L}\cdot\frac{\partial F_2(\theta)}{\partial\theta}\omega(t)-\frac{E}{L_0}(1+f)V_r(t)$$

Where

$$\xi(t)=\int(V_{i+1}-v_i)\,dt$$

$$T_s(\theta)=\frac{1}{g_L}(L_l\cdot g\cdot\rho\cdot w\cdot h\cdot L_0\cdot\cos\theta)$$

$$T_L(\theta)=\frac{1}{g_L}(g\cdot W_L\cdot L_w\cos(\theta+\theta_{lp}))$$

$$F_2(\theta)=[(r-H_0+L_l\cdot\sin\theta)^2+(a+L_l\cdot\cos\theta)^2]^{\frac{1}{2}}+[(r-H_0+L_l\cdot\sin\theta)^2+(L_0-a-L_l\cdot\cos\theta)^2]^{\frac{1}{2}}$$

$$F_3(t_f)=\frac{1}{g_L}t_f\cdot w\cdot h\cdot(L_l\cdot\sin\theta+r)\cdot\{\sin(\theta+\theta_2)-\sin(\theta-\theta_1)\}$$

$$\dot{\xi}(t)=(1+f)V_r(t)+K_{10}t_f(t)$$

$$K_{10}=\left(\frac{dv_i}{dt_f}+\frac{dV_{i+1}}{dt_f}\right)$$

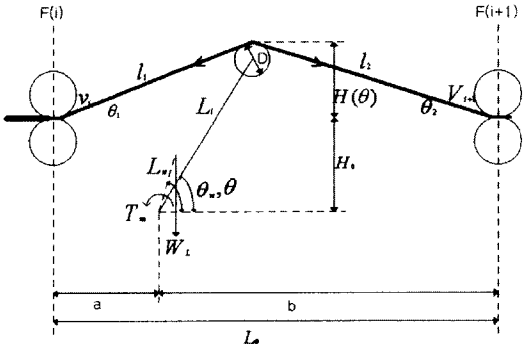

Fig. 2 I-th looper geometry

and the notations are

t_f : Strip tension
E : Young's modulus of the strip
L_0 : Length between stands
θ : Looper angle
g_L : Gear ratio of the looper motor
ω : Looper motor velocity
J_L : Inertia (acting to the looper motor)
z : Damping coefficient
τ : Looper motor torque
τ_{ref} : Reference looper motor torque
T_2 : Looper motor time constant
T_v : Main motor time constant
V_r : Main motor speed
V_{r_ref} : Reference main motor speed
L_1 : Looper arm length
g : Gravity acceleration
ρ : Strip density
w : Strip width
h : Strip thickness
r : Looper roll radius
H_0 : Height from looper motor shaft to stand shaft
V_i : Work roll speed
a : Length from i-th stand to looper shaft
b : Length from (i+1)-th to looper shaft
W_L : Total mass of looper
L_w : Length to looper weight center
θ_w : Interval angle of weight center.
T_{LW} : Torque produced by looper arm and roll

And from the above results, the block diagram of the looer system is shown in Fig. 3. The linear dynamic equations, Eq. (1), for the i-th stand are

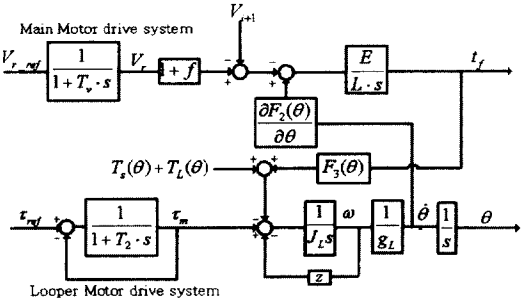

Fig. 3 Block diagram of the looper system for i-th stand

obtained by linearization of the above results, near the operating point of the system.

$$\dot{x}=Ax+Bu$$
$$y=Cx \tag{1}$$

where

$$x=\begin{bmatrix} t_f \\ \theta \\ \omega \\ \tau \\ V_r \end{bmatrix}=\begin{bmatrix} \text{tension of strip} \\ \text{angle of looper} \\ \text{velocity of looper} \\ \text{torque of looper motor} \\ \text{velocity of main motor} \end{bmatrix}$$

$$u=\begin{bmatrix} V_{r\_ref} \\ \tau_{ref} \end{bmatrix}=\begin{bmatrix} \text{roll speed reference} \\ \text{torque reference} \end{bmatrix}$$

$$y=\begin{bmatrix} t_f \\ \theta \end{bmatrix}=\begin{bmatrix} \text{tension of strip} \\ \text{angle of looper} \end{bmatrix}$$

and

$$A=\begin{bmatrix} -\frac{E}{L_0}K_{10} & 0 & \frac{E}{L_0 \cdot g_L}\frac{\partial^2 F_2(\theta)}{\partial \theta^2} & 0 & -\frac{E}{L_0}(1+f) \\ 0 & 0 & \frac{1}{g_L} & 0 & 0 \\ -\frac{1}{J_L}\frac{\partial F_3(t)}{\partial \theta} & -\frac{1}{J_L}\left(\frac{\partial T_L(\theta)}{\partial \theta}+\frac{\partial T_s(\theta)}{\partial \theta}\right) & -\frac{z}{J_L} & \frac{1}{J_L} & 0 \\ 0 & 0 & 0 & -\frac{1}{T_2} & 0 \\ 0 & 0 & 0 & 0 & -\frac{1}{T_v} \end{bmatrix}$$

$$B=\begin{bmatrix} 0 & 0 \\ 0 & 0 \\ 0 & 0 \\ 0 & \frac{1}{T_2} \\ -\frac{1}{T_v} & 0 \end{bmatrix},\quad C=\begin{bmatrix} 1 & 0 & 0 & 0 & 0 \\ 0 & 1 & 0 & 0 & 0 \end{bmatrix}$$

We can know that the single stand system is a MIMO (Multi Input Multi Output) system from Eq. (1).

2.2 Finishing mill set up (FSU)

Now we will explain the finishing mill set up process. In brief, FSU means setting the operation conditions such as strip thicknesses, roll speed, roll gap, slip ratios, looper angles, and so on, to produce proper strip width. To understand FSU, we need to explain the rolling phenomenon.

Figure 4 shows that the strip tension between stands is influenced by the difference of the speed between the i-th and (i+1)-th stand (Shin and Hong, 1998). In addition, the strip speed is different from the work roll speed due to the tension of the i-th stand, i.e. a slip between the roll and strip occurrs. So, the strip speed at the exit of the i-th stand is represented as $v_i=(1+f_i)\,V_R^i$, where f_i is defined as the forward slip ratio for the i-th stand. Similarly, the strip speed at the entrance of the i+1-th stand is represented as $V_{i+1}=(1-\Phi_{i+1})\,V_R^{i+1}$, where the Θ_i is defined as the backward slip ratio for the i-th stand. Further, the equation $H_{i+1}V_{i+1}=h_{i+1}v_{i+1}$ is called the mass-flow constant law. So, the difference of the speed in the i-th stand ($v_e=v_i-V_{i+1}$) is represented as follows,

$$v_e=\left[(1+f_i)-\frac{h_{i+1}}{H_{i+1}}(1+f_{i+1})\frac{V_R^{i+1}}{V_R^i}\right]V_R^i \tag{2}$$

The difference of the speed in the i-th stand can be obtained by the forward slip ratio only, because the strip thickness and the roll speed are established at the set-up process. But in the actual process, the forward slip ratio and backward slip ratio are functions of the diameter of the work roll, the reduction ratio of the thickness, yield stress, friction coefficient, temperature, and so on. They are nonlinear and complex. So in this paper,

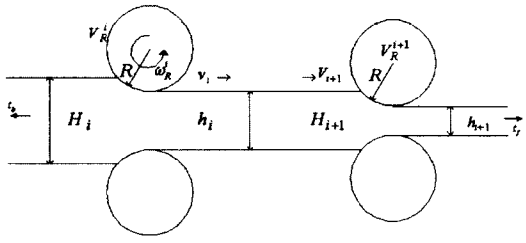

f_i : i[th] stand Forward Slip
ϕ_i : i[th] stand Backward Slip
R : work roll radius
V_R^i : i[th] work roll linear velocity ($=R\omega_R^i$)
H_{i+1}: (i+1)[th] stand entranec strip thickness
h_{i+1} : (i+1)[th] stand exit strip thickness
V_{i+1} : (i+1)[th] stand strip speed
v_{i+1} : (i+1)[th] stand strip speed

Fig. 4 The rolling phenmenon of work rolls

the experimental setting values, obtained in the actual process, will be used.

To describe the finishing mill process fully, it is necessary to set the thickness of the strip, tension, rolling pressure, looper angle, strip speed, roll speed and so on, for each stand. We call this procedure the Finishing mill Set Up (FSU). To realize the rolling process, we will use the value adopted in a real plant.

To complete the full model, the speed of the work roll at the (i+1)th stand needs to have feedback to the i-th stand. The full model is obtained by putting FSU values of Table 1 to the dynamic equation. Each controller with a good performance for each stand is designed by each state equation. The model of the full stand hot strip finishing mill in Fig. 5 is obtained by combining the model of each stand.

Table 1 The values of parameters of i-th stand

	F1	F2	F3	F4	F5	F6	F7
H_i [mm]	32.8	16.3	9.35	5.96	4.2	3.13	2.53
h_i [mm]	16.3	9.35	5.96	4.2	3.13	2.53	2.27
t_b [N/mm^2]	0	4	4.9	6.1	7.1	8.6	10
t_f [N/mm^2]	4	4.9	6.1	7.1	8.6	10	0
Looper angle [degree]		20	19	18	18	18	17
V_R^i [mm/sec]	5500	6000	6500	7000	7500	8072	100000
f_i	3	3	3	8	8	8	8

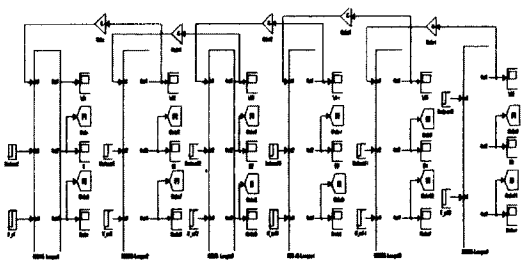

Fig. 5 Block diagram of the hot strip finishing mill

3. Controller Design

In today's steel plant, problems may be encountered using higher order controllers such as LQ, LQG and H_∞. These problems can be overcome by using the PID controller whose design is simple and easily adaptable to existing plant. Therefore, we will discuss the properties of some PID controls and their advantages for use in the finishing mill.

3.1 Conventional PI control

Most finishing mills use PI controllers, so we will review the properties of PI controllers. The appropriate PI controller gain is selected after substituting variables of each stand linearized

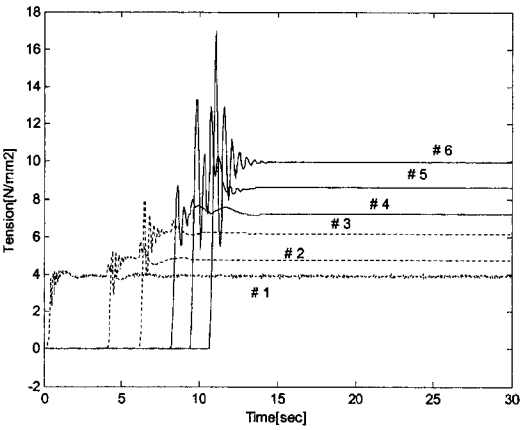

(a) Tension

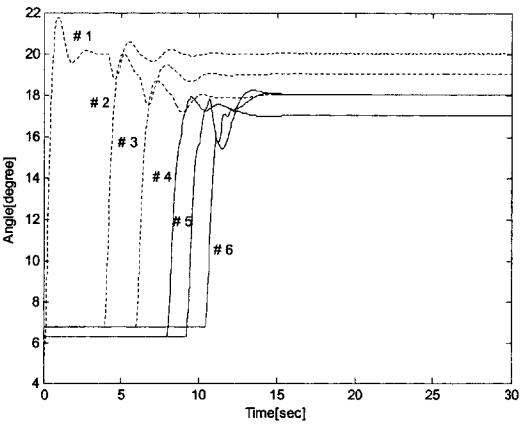

(b) Looper angle

Fig. 6 Simulation result of PI control

from the non linear block diagram, as in Fig. 3. The linearized model is previously represented by the Eq. (1). The control system was designed for a linear system but non linear system simulations were performed to simulate more real conditions. Figure 6 shows the simulation result for the non-linear model in Fig. 5, for the full stand finishing mill system. In Fig. 6, we could see that the overshoots of both tension and angle have increased to that of the linear model at all the stands. The result of the nonlinear system is represented here. That of the linear model is less meaningful. This fact may be caused by the ignored dynamics in the linearization.

Irregular width may occur in the strip through excessive tension. For regular strip width, the overshoots must be decreased at the initial interval of time. In examining the above results, we discovered the interaction between the tension and the looper angle, i.e. the tension fluctuates through the looper angle, and vice versa.

3.2 Cross PI control

To reduce the overshoots, cross gain can be utilized. Furthermore, this method can reduce the interactions between the tension and the looper. Figure 7 is the block diagram for the cross control scheme. Now we describe the method to determine the cross control gains. The transfer function matrix is obtained from Eq. (3) and the block diagram, in Fig. 7.

$$\begin{bmatrix} t_f \\ \theta \end{bmatrix} = \begin{bmatrix} G_{11} & G_{12} \\ G_{21} & G_{22} \end{bmatrix} \begin{bmatrix} V_{ref} \\ T_{ref} \end{bmatrix} \tag{3}$$

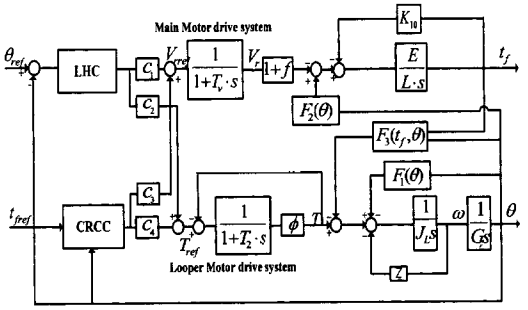

Fig. 7 Block diagram of the Cross control of i-th stand

And Eq. (3) can be expressed as Eq. (4) by substituting $V_{ref} = C_1 \cdot V_{LHC} + C_3 \cdot T_{CRCC}$ and $T_{ref} = C_2 \cdot V_{LHC} + C_4 \cdot T_{CRCC}$.

$$\begin{bmatrix} t_f \\ \theta \end{bmatrix} \begin{bmatrix} G_{11} & G_{12} \\ G_{21} & G_{22} \end{bmatrix} \begin{bmatrix} C_1 & C_3 \\ C_2 & C_4 \end{bmatrix} \begin{bmatrix} V_{LHC} \\ T_{CRCC} \end{bmatrix} \tag{4}$$

where C_i are cross gains in Fig. 7, LHC (Looper Height Controller) controls Looper angle and $CRCC$ (Current Reference Calculation Controller) controls the looper motor torque. The V_{LHC} is the main motor speed control input through the LHC and T_{CRCC} is the looper motor torque control input through the $CRCC$.

Cross control solves the problem of selecting gains $C_i (i = 1 \sim 4)$ with the minimizing of interaction through two control inputs. There are many combinations of coefficients to select them. To simplify the problem, let C_1 and C_4 be 1. This is applicable to the real plant systems because C_1 and C_4 can be implemented in the LHC and $CRCC$.

$$\begin{bmatrix} t_f \\ \theta \end{bmatrix} = \begin{bmatrix} G_{11} & G_{12} \\ G_{21} & G_{22} \end{bmatrix} \begin{bmatrix} 1 & C_3 \\ C_2 & 1 \end{bmatrix} \begin{bmatrix} V_{LHC} \\ T_{CRCC} \end{bmatrix} \tag{5}$$

Then, Eq. (5) can be expressed Eq. (6).

$$\begin{bmatrix} t_f \\ \theta \end{bmatrix} = \begin{bmatrix} G_{11} + G_{12}C_2 & G_{11}C_3 + G_{12} \\ G_{21} + G_{22}C_2 & G_{21}C_3 + G_{22} \end{bmatrix} \begin{bmatrix} V_{LHC} \\ T_{CRCC} \end{bmatrix} \tag{6}$$

In the Eq. (6), $G_{11}C_3 + G_{12}$ and $G_{21} + G_{22}C_2$ should be approximately zero in order to prevent interaction between each output, tension and looper angle. So, if we can make $C_3 = -G_{12}/G_{11}$ and $C_2 = -G_{21}/G_{22}$, we can decouple tension and looper angle in the linear model. However complete decoupling may be impossible because our system is non-linear.

Remember that C_2 and C_3 are functions of the frequency as shown in the above results. But to apply the controller to an actual plant, we should find them as constant coefficients and each gain can be obtained by the final value theorem. In another expression, we can obtain the gains by $\lim_{t \to \infty} C_i(t) = \lim_{s \to 0} sC_i(s)$ under the condition that $sC_i(s)$ is analytic in the right s-plane of the including the imaginary axis. The looper system

satisfies the above condition, so we can obtain the gains easily.

When we selected these constant values through this method, we assumed that the results would not be efficacious because the gains are not frequency dependent. But in Fig. 8, we can see that the results are more effective than anticipated. The simulation results in Fig. 8 are those of cross control decoupling interactions between the tension and looper angle. It is efficacious in reducing the overshoot and to decouple them for each stand, as in Fig. 8. All the overshoots are, compared to conventional PI control, reduced in tension. In general, the strip width defect occurred in front of the strip and tension overshoot is one of the main problems. So the decreasing of overshoot is desirable. Compared to convention PI control, overshoots of the tension were decreased, at the same time, overshoots of the angle were properly maintained. This is the result of a reduced interaction between the tension and the looper angle by using cross gains.

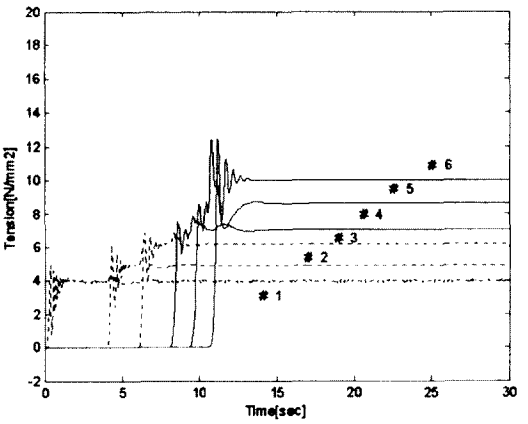

(a) Tension

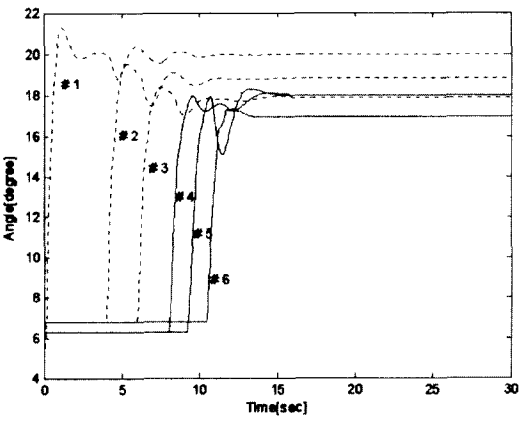

(b) Looper angle

Fig. 8 Simulation result of Cross control

3.3 CDM (Coefficient Diagram Method)

CDM is one of the methods for a controller design using a polynomial approach. Basically, it is a technique to arrange the poles of the closed loop transfer function, in order to get desirable response in the time domain. The suitable pole arrangement can be obtained by using two design parameters, stability index and equivalent time constant. The coefficient diagram is a semi-log plot where the coefficients of the characteristic polynomial for closed loop transfer function are shown in the ordinate in logarithmic scale. And each order of characteristic polynomial is shown in the abscissa. The CDM can consider the response of the time domain in controller design process ; furthermore, the process of the controller design is very systematic. Figure 9 is the block diagram for the CDM. From Fig. 9, the closed loop transfer function is defined as

$$\frac{y}{y_r}=C(s)=\frac{F(s)N(s)}{P_c(s)} \tag{7}$$

and the characteristic polynomial is

$$\begin{aligned} P_c(s) &= A(s)D(s)+B(s)N(s) \\ &= a_n s^n + a_{n-1}s^{n-1}+\cdots+a_1 s+a_0 \end{aligned} \tag{8}$$

And the stability index (γ_i), the equivalent time constant (τ) and the stability limit (γ_i^*) are defined as

$$\gamma_i=\frac{a_i^2}{(a_{i-1}a_{i+1})}, \text{ for } i=1, \cdots, n-1 \tag{9}$$

$$\tau=\frac{a_1}{a_0} \tag{10}$$

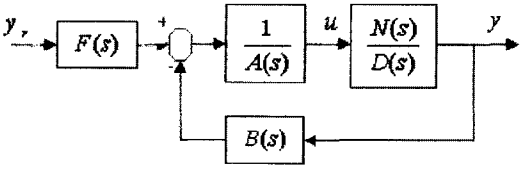

Fig. 9 Block diagram of CDM

$$\gamma_i^* = \frac{1}{\gamma_{i+1}} + \frac{1}{\gamma_{i-1}},\ \gamma_0 = \gamma_n = \infty \tag{11}$$

From the above equations, the following results are derived.

$$a_i = \frac{a_0 \tau^i}{(\gamma_{i-1}\gamma_{i-2}^2 \cdots \gamma_2^{i-2}\gamma_1^{i-1})} \tag{12}$$

We can know that the coefficient of Eq. (8) is calculated by a choice of stability characteristic and equivalent time constant which are design parameters. When the controller using the CDM is designed to obtain the unique solution of Eq. (8), the controller degree must satisfy the next Eq. (13) in Fig. 9.

$$\deg(B) = \deg(D) - 1,\ \deg(A) \geq \deg(B) \tag{13}$$

Where, the $\deg(\bullet)$ means the degree of polynomial of $\bullet$. That means that a high order controller is required for a high order system. Applying the CDM to the PID controller, the $A(s)$, $B(s)$, $F(s)$ in Fig. 9 must be chosen in Fig. 10. To obtain the same structure as a general PID controller, each variable means proportion gain (K_p), integral gain (K_i) and differential gain (K_d). In the calculation of the gains for the PID controller in Fig. 10, a problem may happen when choosing the gain depending on the order of the plant. The problem is that we cannot satisfy Eq. (13) because the equation must be $\deg(B(s)) = 2$ and $\deg(A(s)) = 1$ in Fig. 9. It means that the unique solution for Eq. (8) cannot be calculated, although both the proper stability index and equivalent time constant are selected properly. A more detailed analysis of this problem will be taken up later. For now, we will apply CDM to consider the interaction between channels and to divide MIMO system into several SISO systems. We can obtain the transfer function matrix in Eq. (14) using the state equation of Eq. (1).

$$\mathbf{G}(s) = C(sI - A)^{-1}B = \begin{bmatrix} G_{11}(s) & G_{12}(s) \\ G_{21}(s) & G_{22}(s) \end{bmatrix} \tag{14}$$

The block diagram which applies the CDM using Eq. (14) is Fig. 11. Figure 11 is the single stand block diagram for the PID controller using the CDM. The interaction function in each channel is defined as Eq. (15).

$$\gamma(s) = \frac{G_{12}(s)\,G_{21}(s)}{G_{11}(s)\,G_{22}(s)} \tag{15}$$

To examine the magnitude of the function, the bode diagram of $\gamma(s)$ is represented in Fig. 12. We can see $\| G_{11}(s)\,G_{22}(s) \| > \| G_{12}(s)\,G_{21}(s) \|$, i.e. the $\gamma(s)$ is relatively small, in all the frequency ranges as shown in Fig. 12. So, we can

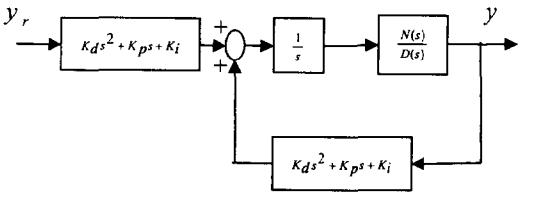

Fig. 10 Block diagram for CDM applied to PID controller

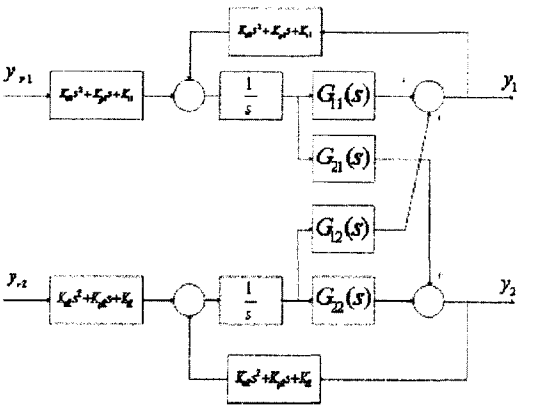

Fig. 11 The single stand's block diagram for the PID controller using the CDM

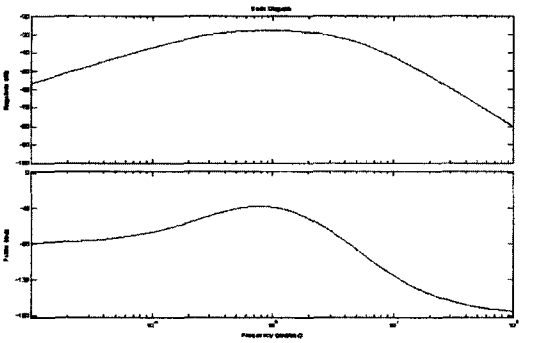

Fig. 12 Bode diagram of $\gamma(s)$

assume that the system can be regarded as the individual SISO system for $G_{11}(s)$ and $G_{22}(s)$. Then we can obtain the PID gains by applying CDM to each SISO system. As the result, the MIMO system is decoupled by using PID gain and we can obtain the simulation results for the system in Fig. 11.

Now we will describe the controller design procedures for the system. First, the controller design for the Main Motor is presented. To describe the design method, we chose the 5th stand. For other stands, the design method is the same. We get the following Eq. (16) and (17) by substituting the actual values for the 5th stand.

$$N(s) = -71.409s^3 - 2698.9s^2 - 15479s - 4986.9 \quad (16)$$

$$D(s) = s^5 + 43.922s^4 + 3010.7s^3 + 88465s^2 + 2.48\times10^5 s + 655.15 \quad (17)$$

The CD (coefficient diagram) for the $D(s)$, the characteristic equation for the open loop transfer function in Eq. (17), is shown in Fig. 13. The characteristic equation for the closed loop transfer function is expressed as follows.

$$P_c(s) = sD(s) + (K_d s^2 + K_p s + K_i)N(s) \quad (18)$$

The above equation can be expressed by Eq. (19).

$$S * K = Co \quad (19)$$

Where,

$$S = \begin{bmatrix} 1 & 0 & 0 & 0 \\ d_4 & n_3 & 0 & 0 \\ d_3 & n_2 & n_3 & 0 \\ d_2 & n_1 & n_2 & n_3 \\ d_1 & n_0 & n_1 & n_2 \\ d_0 & 0 & n_0 & n_1 \\ 0 & 0 & 0 & n_0 \end{bmatrix}, \quad K = \begin{bmatrix} 1 \\ K_d \\ K_p \\ K_i \end{bmatrix}$$

$$Co = \left[\frac{\tau^6}{(\gamma_5^1\gamma_4^2\gamma_3^3\gamma_2^4\gamma_1^5)} \quad \frac{\tau^5}{(\gamma_4^1\gamma_3^2\gamma_2^3\gamma_1^4)} \quad \frac{\tau_4}{(\gamma_3^1\gamma_2^2\gamma_2^3)} \quad \frac{\tau^3}{(\gamma_2^1\gamma_1^2)} \quad \frac{\tau^2}{(\gamma_1^1)} \quad \tau \; 1 \right]^T$$

d_i : the coefficient of i-order of the $D(s)$
n_i : the coefficient of i-order of the $N(s)$

We can know that the problem is the controller order in Eq. (18), as referred previously. As the matrix S in Eq. (19) is not a square matrix, Eq. (19) can not have the unique solution. To solve it, we used the pseudo inverse method. And, we will apply the result of the Manabe standard type (Manabe, 1998) for CDM. First, the stability index (γ_i) called the Manabe standard type in Eq. (20) is used, and the equivalent constant time (τ) is selected for proper value by trial and error method.

$$\gamma = [2.5 \; 2 \; 2 \; 2 \; 2] \quad (20)$$

Then the coefficients of the characteristic polynomial can be obtained by solving Eq. (19). And, the step response and the CD that are obtained

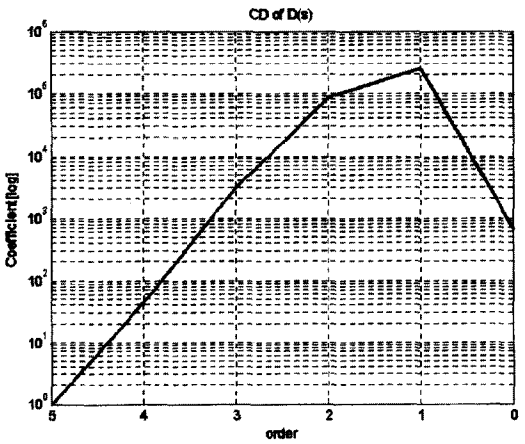

Fig. 13 The CD for $D(s)$

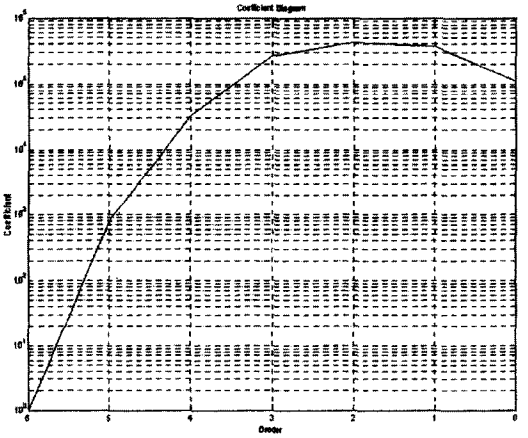

Fig. 14 The CD of $P_c(s)$ using the manabe standard type (Main Motor)

by the process are shown in Fig. 14 and Fig. 15, respectively.

In Fig. 14, the shape of CD is a very desirable convex form but the equivalent time constant has a limitation for selecting the proper solution (stable pole) of Eq. (18). The result shows a very slow response in Fig. 15. The PID gain which is obtained by the standard Manbe method is a small K_P relatively. For these reasons, the step response is slow. To obtain a more desirable response, a setting of the stability index will be performed. The value of K_P for the PID must be increased to get a faster response. So we tuned the gain relatively large, and the step response result is shown in Fig. 16. As the PID gain is newly chosen, the coefficient of the polynomial $P_c(s)$ is perfectly obtained, and the CD for the new polynomial $P_c(s)$ is shown in Fig. 17. From the coefficient of the $P_c(s)$, we can get a new stability index (γ) and stability limit index (γ^*). The results are as follows.

$$\gamma=[5.0241\ 11.2382\ 2.6\ 3.2755\ 1.7692\ 0.6048]$$

$$\gamma^*=[0.0896\ 0.4583\ 0.3819\ 0.3015\ 0.2923]$$

Next, the PID controller for the looper motor was designed by the same method as the main motor. The result of the CD is shown in Fig. 18.

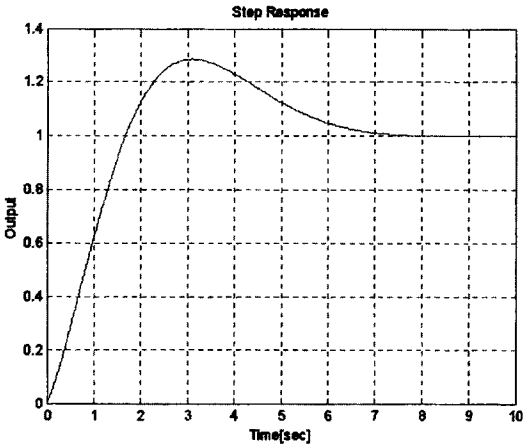

Fig. 15 The step response with the manabe standard type (Main Motor)

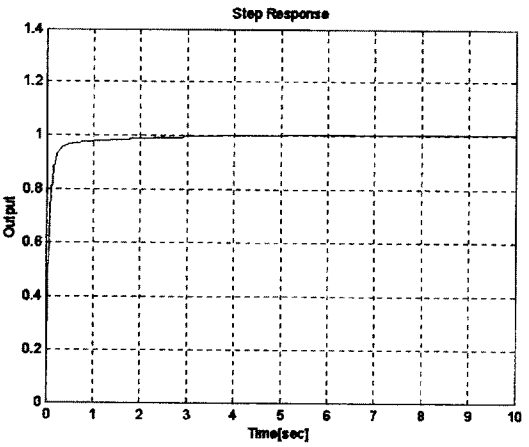

Fig. 16 The step respones after setting the standard index (Main Motor)

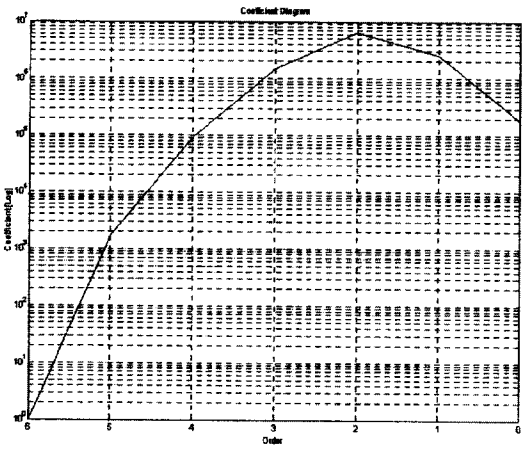

Fig. 17 The CD after setting the stability index (Main Motor)

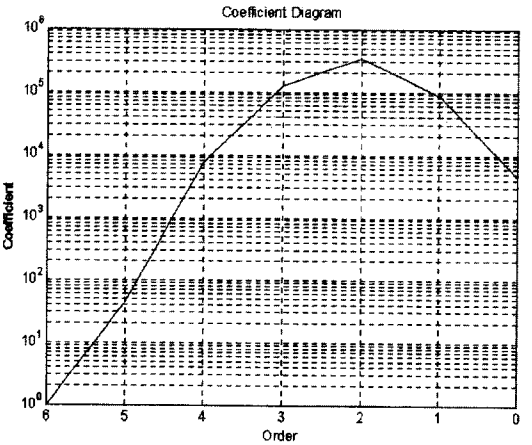

Fig. 18 The CD of the looper motor using PID

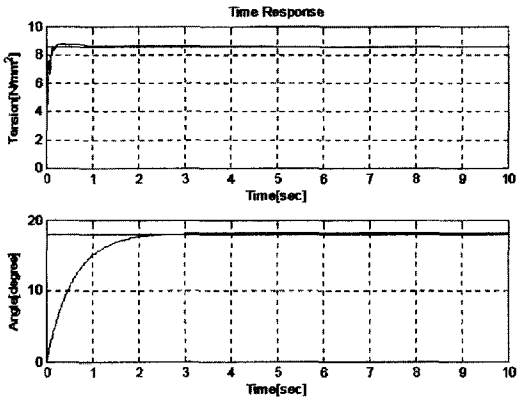

Fig. 19 The step response of the 5th stand (linear model)

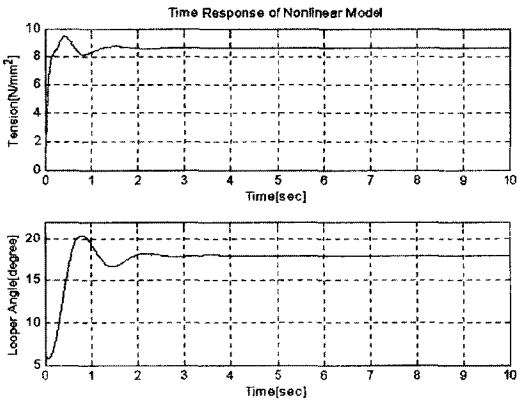

Fig. 20 The step response of the 5th stand (non-linear model)

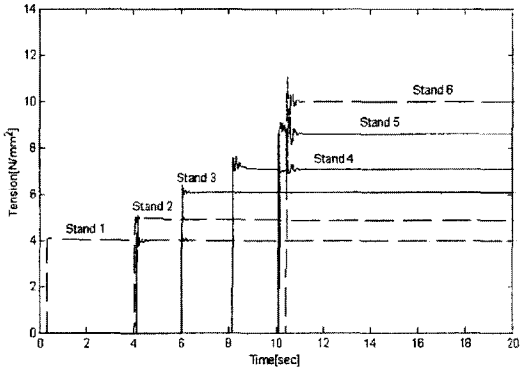

(a) Tension

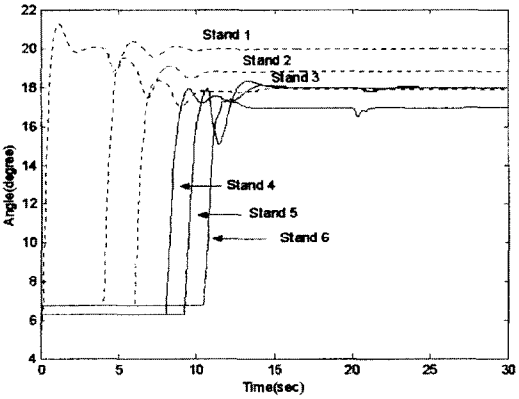

(b) Looper angle

Fig. 21 The simulation result of PID-CDM

The overall results for CDM are represented in Fig. 19. Figure 19 is the step response using the CDM PID controller in the linear model for the 5th stand. Figure 20 is the step response using the CDM PID controller in the non-linear model for the 5th stand. The effects of the ignored dynamics may happen in each stand due to the difference between the non-linear system and the linear system. Fairly good results can be obtained from the CDM. The stability index for the 5th stand can be applied to all stands to consider parameter change as disturbance. This may yield good data, demonstrating the robustness of CDM. The next simulation result in Fig. 21 is that of the full stand with the CDM PID controller. We can see better results compared to that of Conventional PI or PI-Cross controller. First of all, the overshoots in tension are decreased as are interactions between tension and the looper. At about 20 seconds, there are slight changes in the looper angle due to the coiling process. But they had no direct effect on previous stand and tension.

4. Conclusion

In hot strip finishing mill, a strip width control is very important point to determine strip quality. The strip width depends on the strip tension. We know that the tension varies due to the difference of the work roll speed and the looper angle. Therefore, we should maintain the uniform tension through controlling the looper angle and the roll speed. However, it is difficult to independently control them because of interaction between them. Thus, hot strip finishing mill process

which reflects the character of each stand was simulated using the linear state equation of the single stand. We investigated simulation results for a non-linear system with several results from the linear system. Furthermore, the simulation result for one stand cannot apply the full finishing mill process because the full process interacts with the other stands. So, we performed simulations for a non-linear full stand model applying several control methods with the real FSU values. In the simulations, actual stands have large overshoot because they have thin strip and high stiffness. As a result, we discovered that Conventional PI Control had large overshoot and interaction between the tension and looper angle. However, we found that PI with Cross Control and CDM more decreased overshoot and interaction between the tension and looper angle. Moreover, a decreased overshoot reduce the strip width defect at the initial time and contribute to improvement of the strip quality.

We well know that simulation results may be different from an actual finishing mill process, but these results for the full stand can be used as prediction programs for finishing mill plans and applied to other control systems. In addition, they can be used in a simulator and a performance-estimate program for hot strip finishing mills.

Acknowledgment

This research was financially supported by the Korea Science and Engineering Foundation (KOSEF) through the Engineering Research Center for Net Shape and Die Manufacturing (ERC/NSDM) at Pusan National University and by Pusan National University Research Grant.

References

Hearns, G. and Grimble, M. J., 1997, "Multivariable Control of a Hot Strip Finishing Mill," *Proceedings of the American Control Conference Albuquerque, New Mexico*, pp. 3775~3779.

Hesketh, T., Jiang, Y. A., Climents, D. J., Butler, D. H. and van der Laan, R., 1998, "Controller Design for Hot Strip Finishing Mills," *IEEE Trans. on Control System Techology*, Vol. 6, No. 2, pp. 208~219.

Man Hyung Lee, 2001, *Development of a High-Precision Automatic Control System for Hot-Strip Mill Finisher*, RIMT, Pusan National University (The last report of first year), in Korea.

Manabe, S., 1997, *An Algebraic Approach to Control System Design; Coefficient Diagram Method*, (Lecture note), Chungbuk National University, in Korea.

Manabe, S., 1998, "Coefficient Diagram Method," *Proc. of 14th IFAC Symposium on Automatic Control in Aerospace*, pp. 199~210.

Masanoti Shioya, Naohatu Yoshitani, and Takatsugu Ueyama, 1995, "Noninteracting Control with Disturbance Compensation and its Application to Tension-Looper Control for Hot Strip Mill," *IEEE*, pp. 229~234.

Myungjun, H., 1998, "A CDM for High-Order Plant," *Proc. of the 13th KACC*, pp. 793~795, in Korea.

Shin, K. H. and Hong, W. K., 1998, "Real-Time Tension Control in a Multi-Stand Rolling System," *KSME International Journal*, Vol. 12, No. 1, pp. 12~21, in Korea.

Young-Chol Kim, 2001, "Application of CDM to MIMO System : Control of Hot Rolling Mill," *Transactions on Control, Automation and Systems Engineering*, Vol. 3, No. 4, pp. 250~256, in Korea.